hydrolytic condensation. To this end, a criterion has been devised for establishing the position of ν(Ti–O) stretching frequencies in titanium(IV) isopropoxide compounds by determining the difference ν(Ti–O-*i*-Pr) – ν(Ti–O-*i*-Pr-d_7), defined here as $\Delta\nu$(Ti–O-*i*-Pr) = 57 cm^{-1}. We envisage that this may be utilized in other systems as a means of unambiguously establishing the position of ν(M–O) stretching frequencies and may aid characterization of metal alkoxide compounds in solution.[22]

During submission of this manuscript, we learned that the single-crystal X-ray diffraction structure of NaTi(O-*i*-Pr)$_5$ was solved on crystals grown from pentane solution at −25 °C. The structure (R = 8.6%) consists of infinite linear chains of alternating tetrahedral sodium and distorted-trigonal-bipyramidal titanium atoms connected by bridging isoproxy groups.[23]

Acknowledgment. We thank Drs. Dan Doughty and Chuck Peden for helpful discussions, Eva Quesnell for typing the manuscript, and the NSF for purchase of an NMR spectrometer under the Chemical Instrumentation Program. This work was financially supported by Sandia National Laboratories, Contract No. 05-2694.

Supplementary Material Available: A full listing of bond lengths and angles, anisotropic thermal parameters, H-atom coordinates, and crystal data (4 pages); a listing of observed and calculated structure factors (7 pages). Ordering information is given on any current masthead page.

(22) ^{13}C NMR data have also been used to examine the solution structures of titanium alkoxide compounds: Holloway, C. E. *J. Chem. Soc., Dalton Trans.* **1976**, 1050.

(23) Bradley, D. C.; Patel, A. Private communication, June 1990.

Contribution from the Institut für Anorganische und Physikalische Chemie, Universität Bern, CH-3000 Bern 9, Switzerland, Laboratorium für Neutronenstreuung, ETHZ, 5303 Würenlingen, Switzerland, and Institut Laue Langevin, 38042 Grenoble Cedex, France

Exchange Interactions in Rare-Earth-Metal Dimers. Neutron Spectroscopy of $Cs_3Yb_2Cl_9$ and $Cs_3Yb_2Br_9$

Hans U. Güdel,*[1a] Albert Furrer,[1b] and Herma Blank[1c]

Received March 8, 1990

The title compounds were synthesized and studied by high-resolution inelastic neutron scattering. Magnetic dimer excitations were measured on polycrystalline samples at 1.8 K. The observed energy splittings of the ground state can be accounted for by a Heisenberg Hamiltonian with antiferromagnetic exchange parameters $2J$ = −3.25 (3) and −2.87 (3) cm^{-1} for $Cs_3Yb_2Cl_9$ and $Cs_3Yb_2Br_9$, respectively.

1. Introduction

A great deal of work has been done toward a better understanding of exchange interactions in dimers of transition-metal ions.[2] In contrast, dimers of rare earth (RE) metal ions have received much less attention, and little is known to date about the nature of magnetic couplings in such species.[3-7] Due to the shielding of magnetic 4f electrons, as compared to 3d electrons in transition metal ion systems, exchange interactions are expected to be considerably smaller in rare-earth-metal systems. This is confirmed by magnetic ordering temperatures below 5 K in rare-earth-metal halides. In addition to exchange interactions, magnetic dipole–dipole interactions are considered to play a crucial role in these magnetic ordering phenomena. Highly anisotropic g values are characteristic of most rare-earth-metal ions in noncubic crystalline environments, and correspondingly, exchange interactions are often represented by Ising or XY operators.[8,9]

It is not a priori clear whether the same effective Hamiltonians can also be used to describe the energetic splittings resulting from exchange interactions in dimers. A Heisenberg Hamiltonian has been found adequate for an interpretation of EPR results obtained for Gd^{3+} dimers in a variety of host lattices.[4,10] This is a special case, however, since the Gd^{3+} ion, with its half-filled 4f shell, has a completely isotropic ground-state $^8S_{7/2}$. On the other hand, evidence of anisotropic exchange as well as contributions from magnetic dipole–dipole interactions was obtained from EPR measurements of Ce^{3+} and Nd^{3+} dimers.[3] The interaction parameters were obtained from the experimental data by rather involved procedures in these investigations.

From a study of a number of transition-metal dimers we have found that inelastic neutron scattering (INS) is a very straightforward technique for the determination of exchange parameters.[11] Transitions between exchange-split components of the ground state are usually observable. These energy splittings can thus be determined in a very direct way, without any complicating effects from external magnetic fields as in EPR or magnetic susceptibility measurements. The INS technique should be equally useful for the study of rare-earth-metal dimers,[12] and we chose the family of compounds with composition $Cs_3(RE)_2Br_9$ (RE = Tb^{3+}, Dy^{3+}, Ho^{3+}, Er^{3+}, Yb^{3+}) for our studies. These compounds all crystallize in space group $R\bar{3}c$, and they contain the dimeric species $(RE)_2Br_9^{3-}$ depicted in Figure 1. The great advantage of such a system compared to one doped with RE ions is the presence of only one magnetic species and thus the absence of overlapping spectra. First results of these studies are reported in refs 12–16. They show that for RE = Tb^{3+}, Dy^{3+}, and Yb^{3+} a Heisenberg model adequately describes the observed splittings as long as only

* To whom correspondence should be addressed.

(1) (a) Universität Bern. (b) ETHZ. (c) Institut Laue Langevin.
(2) *Magneto-Structural Correlations in Exchange Coupled Systems*; Willett, R. D., Gattschi, D., Kahn, O., Eds.; D. Reidel: Dordrecht, The Netherlands, 1985.
(3) Riley, J. D.; Baker, J. M.; Birgenau, R. J. *Proc. R. Soc. London* **1970**, *A320*, 369.
(4) Cochrane, R. W.; Wu, C. Y.; Wolf, W. P. *Phys. Rev. B* **1973**, *8*, 4348.
(5) Wolf, W. P. *J. Phys.* **1971**, *C1*, 26.
(6) Velter-Stefanescu, M.; Nislor, S. V. *Phys. Rev. B* **1986**, *34*, 1459.
(7) Maedra, A.; Sugimoto, H. *J. Chem. Soc., Faraday Trans. 2* **1986**, *82*, 2019.
(8) De Jongh, L. J.; Miedema, A. R. *Adv. Phys.* **1974**, *23*, 1.
(9) Carlin, R. L. *Magnetochemistry*; Springer: Berlin, 1986.
(10) Cochrane, R. W.; Wolf, W. P. *Solid State Commun.* **1971**, *9*, 1997 and refs 2–5 therein.
(11) Güdel, H. U.; Furrer, A.; Kjems, J. K. *J. Magn. Magn. Mater.* **1986**, 54–57, 1453 and references therein.
(12) Furrer, A.; Güdel, H. U.; Darriet, J. *J. Less-Common Met.* **1985**, *111*, 223.
(13) Dönni, A.; Furrer, A.; Blank, H.; Heidemann, A.; Güdel, H. U. *J. Phys.* **1988**, *C8*, 1513.
(14) Dönni, A.; Furrer, A.; Blank, H.; Heidemann, A.; Güdel, H. U. *Physica B* **1989**, *156 + 157*, 370.
(15) Furrer, A.; Güdel, H. U.; Blank, H.; Heidemann, A. *Phys. Rev. Lett.* **1989**, *62*, 210.
(16) Furrer, A.; Güdel, H. U.; Krausz, E. R.; Blank, H. *Phys. Rev. Lett.* **1990**, *64*, 68.

0020-1669/90/1329-4081$02.50/0

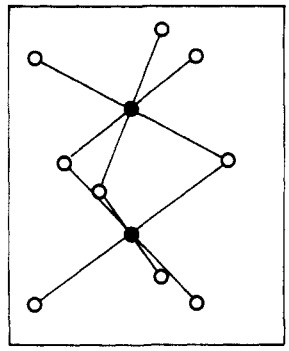

Figure 1. Schematic structure of the $Yb_2Cl_9^{3-}$ and $Yb_2Br_9^{3-}$ dimers.

one crystal field state is considered.[13-15] For RE = Ho^{3+} it was found that for a proper reproduction of the observed splittings in three crystal field states an exchange-tensor formalism was most appropriate.[16]

The title compounds were chosen because they are isostructural, and the effect of the chemical variation on the exchange splittings can thus be directly interpreted. In addition, Yb^{3+} is a special case with only one electron missing in the closed 4f shell. Magnetic susceptibility measurements on $Cs_3Yb_2Cl_9$ and $Cs_3Yb_2Br_9$ in the temperature range 4.2–1.0 K, which were recently reported, revealed that such measurements are very sensitive to small amounts of impurities.[17] The typical broad maximum in χ versus T expected for an antiferromagnetically coupled dimer system could be observed in only one of three samples of $Cs_3Yb_2Br_9$ but not in $Cs_3Yb_2Cl_9$. Impurities of the order of 1% are very difficult to avoid in these compounds, but they do not affect the results obtained by INS. In the following we present experimental results and discuss the exchange splittings thus obtained.

2. Experimental Section

Polycrystalline samples of $Cs_3Yb_2Cl_9$ and $Cs_3Yb_2Br_9$ were obtained by a slight modification of the general procedure given in ref 18. Yb_2O_3 (puriss 99.9%, Fluka), CsCl (suprapur, Merck) and CsBr (suprapur, Merck), and HCl (30%, suprapur, Merck) and HBr (47%, suprapur, Merck) were used as starting materials. The HCl and HBr treatments were carried out at 500 °C. The samples were checked by powder X-ray diffraction. They showed the correct pattern, and impurity lines accounted for less than 2% of the intensity. Platelike aluminum containers of dimensions 45 × 40 × 4 mm^3 were used for the INS experiments. In the $Cs_3Yb_2Br_9$ samples used in this study, 10% of the Yb^{3+} ions were replaced by Dy^{3+} and Cr^{3+} ions, respectively. They were synthesized for the purpose of studying Yb^{3+}–Dy^{3+} and Yb^{3+}–Cr^{3+} dimer excitations, which will be reported elsewhere. These samples proved to be very suitable for studying the prominent Yb^{3+}–Yb^{3+} excitations as well.

Inelastic neutron scattering experiments were done at the Institut Laue Langevin in Grenoble, France, on the time-of-flight instruments IN5 and IN6 using cold neutrons. Wavelengths of 6.5 and 8 Å were used on IN5, and a wavelength of 5.9 Å was used on IN6. Scattering angles covered a range of 2 to 134° on IN5 and 10 to 115° on IN6. The samples were placed in a He cryostat with the incident neutron beam hitting the Al container at a 45° angle.

3. Results

Figure 2 shows low-temperature energy spectra of neutrons scattered from polycrystalline $Cs_3Yb_2Cl_9$ and $Cs_3Yb_2Br_9$ for the total range of scattering angles. These data were obtained with IN6. Inelastic features are observed both in energy loss (left-hand side) and energy gain (right-hand side). These correspond to the Stokes and anti-Stokes regions in Raman spectroscopy. The prominent inelastic peaks are due to $Yb_2Cl_9^{3-}$ and $Yb_2Br_9^{3-}$ excitations. The following peak positions are obtained at 2 K:

$Cs_3Yb_2Cl_9$	3.25 (3) cm^{-1}
$Cs_3Yb_2Br_9$	3.00 (3) cm^{-1}
$Cs_3Yb_2Br_9$ (10% Dy)	2.87 (3) cm^{-1}
$Cs_3Yb_2Br_9$ (10% Cr)	2.86 (3) cm^{-1}

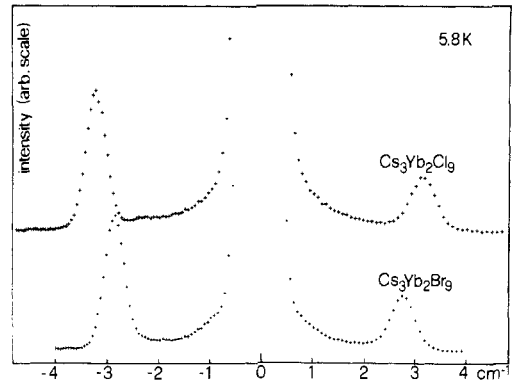

Figure 2. Energy spectra of neutrons scattered from $Cs_3Yb_2Cl_9$ and $Cs_3Yb_2Br_9$ with 10% Cr^{3+} at 5.8 K. Conditions: instrument IN6 at ILL Grenoble; total of all scattering angles; wavelength 5.9 Å.

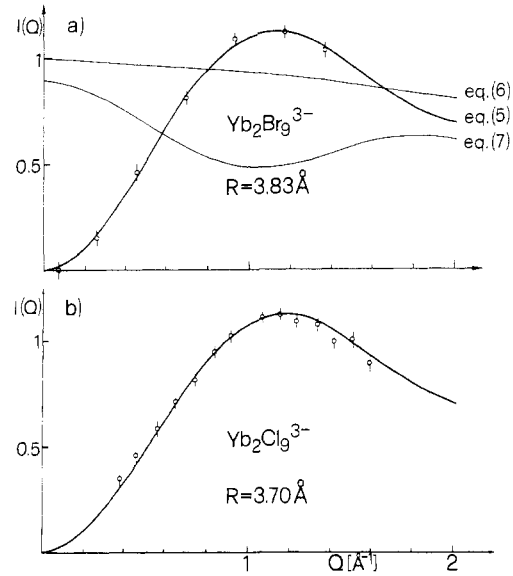

Figure 3. Observed (circles with estimated error bars) and calculated (lines) Q dependence of the inelastic peak intensity at 1.8 K. The strong lines are fits of eq 5 with a scaling factor as adjustable parameter. In (a) the functions of eqs 6 and 7 are included as thin lines for comparison.

The measurements on the undoped $Cs_3Yb_2Br_9$ were made earlier on a backscattering instrument. We attribute the difference in the excitation energy relative to that measured for the doped samples to an instrumental artifact, so that we take 2.87 cm^{-1} as a typical excitation energy of $Cs_3Yb_2Br_9$. The excitation energy is thus about 10% higher in the chloride than the bromide.

The intensity, but not the position, of the inelastic peaks is very strongly dependent on the scattering angle. In Figure 3 the intensities of the energy loss peaks in the two compounds are plotted as a function of the modulus of the scattering vector $\vec{Q}$. $\vec{Q}$ is the difference vector between the wave vectors of scattered ($\vec{k}$) and incoming ($\vec{k}_0$) neutrons. The observed Q dependence is very characteristic of magnetic dimer excitations, as will be analyzed in detail in section 4.2. The time-of-flight instruments IN5 and IN6 are particularly suited for such studies, because they allow measurements down to very low Q values, 0.05 $^{-1}$ for IN5 and 0.2 $Å^{-1}$ for IN6.

The temperature dependence in the range 1.8–14.4 K is very pronounced in the spectra of both compounds. Figure 4 shows the results for $Cs_3Yb_2Cl_9$, both energy loss and energy gain inelastic peaks.

4. Data Analysis

4.1. Ground-State Splitting. Yb^{3+} has a $4f^{13}$ electron configuration with a $^2F_{7/2}$ free ion state lowest in energy. $^2F_{5/2}$ lies some 10 000 cm^{-1} higher. An octahedral crystal field splits $^2F_{7/2}$ into three crystal field states, as depicted in Figure 5. The ground state is a Kramer's doublet, and it is separated from the next higher

(17) Carlin, R. L.; Merabet, K. E.; Shum, D. P.; Darriet, J.; Güdel, H. U. *J. Appl. Phys.* **1990**, *67*(9), 5855–5856.
(18) Meyer, G. In *Inorganic Syntheses*; Holt, S. L., Ed.; Wiley: New York, 1983; Vol. 22, p 1.

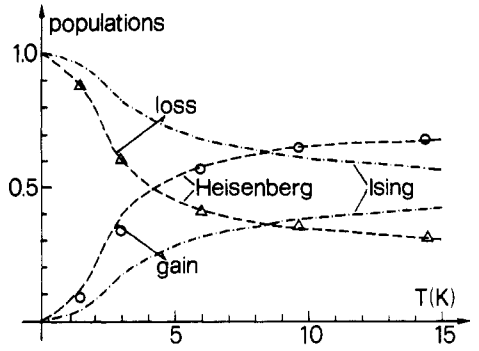

Figure 4. Experimental (triangles for energy loss, circles for energy gain) and calculated (lines) temperature dependence of inelastic peak intensity in $Cs_3Yb_2Cl_9$ for Heisenberg and Ising models, respectively. The intensities were scaled to fit the Heisenberg curve at 1.5 K (loss) and 14.4 K (gain).

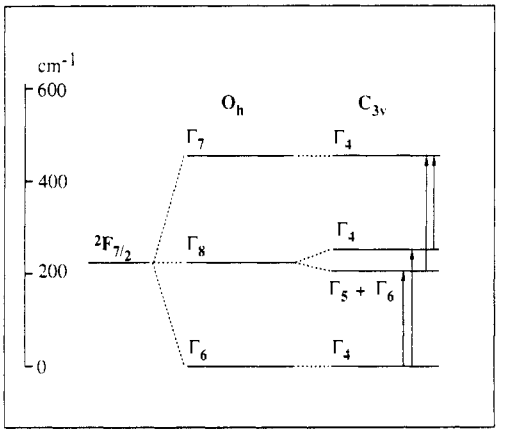

Figure 5. Splitting of Yb^{3+} ground state in octahedral and trigonal crystal fields. Allowed and observed INS transitions are shown by arrows. The ordinate scale is appropriate for $Cs_3Yb_2Br_9$.

state by more than 200 cm^{-1}. This crystal field splitting was earlier determined for $Cs_3Yb_2Br_9$ by INS; the corresponding transitions are shown as arrows in Figure 5.[12]

In Yb^{3+}-doped Cs_2NaYCl_6, in which Yb^{3+} occupies an exactly octahedral position, a g value of 2.84 was experimentally determined, quite close to the calculated value of 2.66 for Γ_6 in O_h. In our dimer there is a strong axial distortion, the single-ion point symmetry is C_{3v}. The dimer symmetry is exactly D_3 but approximately D_{3h}, and we use this latter approximation for the designation of dimer levels in Figure 5. From the crystal field wave functions we calculate $g_\parallel = 2.63$ and $g_\perp = 2.70$. Exchange interactions represent a very small perturbation of the crystal field levels. We can thus consider the Yb^{3+} single-ion ground state as an effective spin-$^1/_2$ state and write the dimer interaction Hamiltonian in the following general form:

$$\hat{\mathcal{H}} = -2J\vec{S}_1\cdot\vec{S}_2 - 2J^z S_1^z\cdot S_2^z \qquad (1)$$

In order to cover the entire range of exchange parameters J and J^z, we introduce the following parametrization:

$$J = Ar \qquad J^z = A(1 - |r|) \qquad (2)$$

i.e., A is a scaling factor and r is a relative measure of the magnitudes of J and J^z. With this notation we have the Heisenberg model for $r = \pm 1$, the Ising model for $r = 0$, and the XY model for $r = {}^1/_2$. Diagonalization of eq 1 gives rise to the energy level diagram shown in Figure 6. Since only one INS transition is observed in our dimers, we must be at either $r = \pm 1$ (Heisenberg), $r = -{}^1/_3$, or $r = 0$ (Ising) in this diagram. These situations can be distinguished on the basis of the Q and T dependence of the corresponding INS transition, as will be shown in the following.

4.2. Inelastic Neutron Scattering. The principle of the technique when applied to dimers and the equations for the scattering cross section of rare-earth-metal dimer excitations have been given in

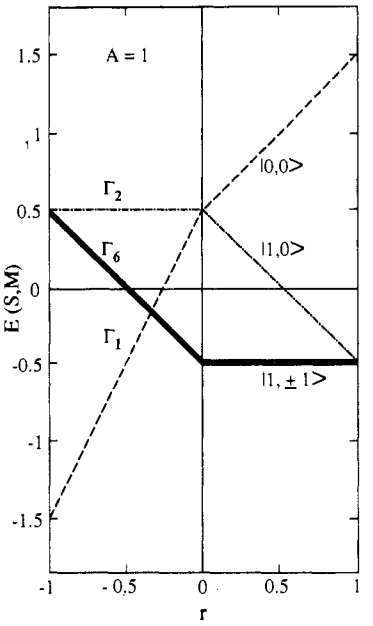

Figure 6. Energy level diagram of an exchange-coupled dimer of spin-$^1/_2$ ions according to eqs 1 and 2.

ref 12. Here we concentrate on those factors in the cross-section formula that depend on the modulus of the scattering vector Q. For $\Delta M = 0$ transitions we get[12]

$$I(Q) \sim F^2(Q)\left\{{}^2/_3 + (-1)^{S-S'}\left[\frac{2\sin(QR)}{Q^3R^3} - \frac{2\cos(QR)}{Q^2R^2}\right]\right\} \qquad (3)$$

and for $\Delta M = \pm 1$ transitions[12]

$$I(Q) \sim F^2(Q)\left\{{}^2/_3 - (-1)^{S-S'}\left[\frac{\sin(QR)}{Q^3R^3} - \frac{\cos(QR)}{Q^2R^2} - \frac{\sin(QR)}{QR}\right]\right\} \qquad (4)$$

R is the separation of the two Yb^{3+} ions in the dimer and $F(Q)$ is the magnetic form factor of Yb^{3+}. The factors in braces are so-called interference terms. On the basis of eqs 3 and 4, we derive the following Q dependences for the three relevant situations in Figure 6:

$$r = \pm 1 \text{ (Heisenberg)} \quad I(Q) \sim F^2(Q)\left[1 - \frac{\sin QR}{QR}\right] \qquad (5)$$

$$r = 0 \text{ (Ising)} \quad I(Q) \sim F^2(Q) \qquad (6)$$

$$r = -{}^1/_3 \quad I(Q) \sim F^2(Q)\left[1 - \frac{2\sin(QR)}{Q^3R^3} + \frac{2\cos(QR)}{Q^2R^2} + \frac{\sin(QR)}{QR}\right] \qquad (7)$$

The three functions are compared with the experimental data of $Cs_3Yb_2Br_9$ in Figure 3a. It is clear that only eq 5 is able to reproduce the experimentally observed drop of the intensity with decreaseing Q. The agreement between the experimental points and the calculated curve with only one adjustable scaling factor is perfect, and the same is true for $Cs_3Yb_2Cl_9$ shown in Figure 3b. We conclude that the exchange splitting in $Cs_3Yb_2Cl_9$ and $Cs_3Yb_2Br_9$ is of the Heisenberg type. This is confirmed by the observed temperature dependence of the inelastic peak intensities. In Figure 4 it is compared with calculated temperature dependences for the Heisenberg and Ising situations, respectively. Clearly, the Ising model can be ruled out also on this basis. In addition, the temperature dependence provides the antiferromagnetic sign of the splitting: a singlet lying below the triplet by an energy $-2J$. We thus get the following isotropic exchange-parameter values ($J^z = 0$ in eq 1):

$Cs_3Yb_2Cl_9$ $2J = -3.25$ (3) cm^{-1}

$Cs_3Yb_2Br_9$ $2J = -2.87$ (3) cm^{-1}

5. Discussion

In most dimeric transition metal ion systems a Heisenberg description is most adequate, and it is usually argued that a complete or partial quenching of the orbital angular momentum is responsible for this. Rare-earth-metal ions, on the other hand, usually have unquenched orbital angular momenta. For the Yb^{3+} systems studied here, the anisotropy of g values in the ground state is not very pronounced. It is therefore not surprising that the exchange splitting in the title compounds can be described by a Heisenberg Hamiltonian. This cannot be generalized, however, as was shown in ref 16 for $Cs_3Ho_2Br_9$. Neither a Heisenberg nor an anisotropic Hamiltonian of the type in eq 1 could account for the observed splittings in three crystal field states. An exchange-tensor formalism was then successfully used.[16,19] A more fundamental treatment has to take explicit account of the orbital functions of the electrons involved in the coupling. There have been numerous theoretical approaches to this,[20] and we are planning to explore some of these models in order to gain a better understanding of the observed exchange splittings in the whole series of $Cs_3(RE)_2Br_9$ dimer compounds.

The difference of approximately 10% between $Cs_3Yb_2Cl_9$ and $Cs_3Yb_2Br_9$ is reminiscent of exchange-coupled transition metal ion systems with face-sharing octahedra. In the dimers $M_2X_9^{3-}$ ($M = Ti^{3+}, V^{3+}, Cr^{3+}$; $X = Cl^-, Br^-, I^-$) it was found that the relative orbital contributions to the exchange parameter J varied greatly upon variation of either the metal ion or the halide ion.[21] In the chloride dimers the dominant contribution was J_{aa}, the orbital parameter involving the trigonal a orbitals on the metal centers, i.e. those orbitals that point directly toward each other. This interaction was strongly reduced in the bromide dimers as a result of the increased metal-metal distance. We conclude, by analogy, that a similar mechanism is responsible for the coupling in the $Yb_2Cl_9^{3-}$ and $Yb_2Br_9^{3-}$ dimers.

Acknowledgment. We are indebted to N. Furer for synthesizing the compounds. Financial support by the Swiss National Science Foundation is gratefully acknowledged.

(19) Levy, P. M. In *Magnetic Oxides*; Craik, D. J., Ed.; Wiley: New York, 1975; Part 1, p 181.

(20) Leuenberger, B.; Güdel, H. U. *Mol. Phys.* **1984**, *51*, 1 and refs 6-18 therein.

(21) Leuenberger, B.; Güdel, H. U. *Inorg. Chem.* **1986**, *25*, 181.

Contribution from the Department of Chemistry and Biochemistry, University of Windsor, Windsor, Ontario, Canada N9B 3P4, and Department of Chemistry, University of Winnipeg, Winnipeg, Manitoba, Canada R3B 2E9

Crown Thioether Ligands Containing Rigid Xylyl Units. Synthesis and Structures of 2,5,8-Trithia[9]-*o*-benzenophane (TTOB), 2,5,8-Trithia[9]-*m*-benzenophane (TTMB), and *fac*-$Mo(CO)_3$(TTOB)·DMSO

Broer de Groot and Stephen J. Loeb*

Received March 15, 1990

The crown thioethers 2,5,8-trithia[9]-*o*-benzenophane (TTOB) and 2,5,8-trithia[9]-*m*-benzenophane (TTMB) were prepared by the reaction of the dipotassium salt of 3-thiapentane-1,5-dithiol with α,α'-dibromo-*o*-xylene and α,α'-dibromo-*m*-xylene, respectively. These compounds were characterized by ^1H and $^{13}C\{^1H\}$ NMR, GCMS, and X-ray crystallography methods. The ortho isomer crystallized in the space group $P2_1/n$, with $a = 8.840$ (2) Å, $b = 15.866$ (5) Å, $c = 10.600$ (2) Å, $\beta = 119.34$ (6)°, $V = 1295.9$ (6) Å^3, and $Z = 4$. The structure was refined to $R = 4.80\%$ and $R_w = 5.51\%$ for 1034 reflections with $F_o^2 > 3\sigma(F_o^2)$. The meta isomer crystallized in the space group $P2_12_12_1$, with $a = 9.107$ (5) Å, $b = 8.851$ (7) Å, $c = 31.90$ (2) Å, $V = 2571$ (1) Å^3, and $Z = 8$. The structure refined to $R = 6.59\%$ and $R_w = 7.04\%$ for 1384 reflections with $F_o^2 > 3\sigma(F_o^2)$. In both structures, the S atoms are exodentate to the ring with a $-SCH_2CH_2SCH_2CH_2S-$ "bracket" bridging the xylyl group and the plane of the aromatic ring approximately perpendicular to the mean plane of the S atoms. Molecular mechanics calculations (MMX) indicated the possibility of a conformation for TTOB, with all S atoms endodentate, which would be ideal for facial coordination to a metal center. The reaction of TTOB with *fac*-$Mo(CH_3CN)_3(CO)_3$ gave the complex *fac*-$Mo(CO)_3$(TTOB), showing that the predicted facial coordination mode is possible in octahedral geometry. The complex *fac*-$Mo(CO)_3$(TTOB)·DMSO crystallized in the space group $P2_1/c$, with $a = 7.732$ (4) Å, $b = 18.69$ (2) Å, $c = 15.00$ (1) Å, $\beta = 104.05$ (6)°, $V = 2103$ (1) Å^3, and $Z = 4$. The structure was refined to $R = 4.52\%$ and $R_w = 5.44\%$ for 2174 reflections with $F_o^2 > 3\sigma(F_o^2)$. The analogous coordination mode for TTMB was neither indicated by molecular mechanics calculations nor observed in similar complexation studies.

Introduction

It is now well established that crown thioethers favor the adoption of "inside-out" or exodentate conformations with the sulfur donor atoms oriented out of the macrocyclic cavity.[1-3] This results from the tendency of $-SCH_2CH_2SCH_2CH_2S-$ chains to adopt a "bracket" structure that prefers anti placements for carbon-carbon bonds and gauche placements for carbon-sulfur bonds.[4] Each thioether molecule must then undergo substantial conformational change in order to attain the "crown" conformation of the macrocycle essential for metal ion coordination.[1-12] The need for these large conformational changes often results in the formation of complexes with limited stability or complexes in which

* Author to whom correspondence should be addressed at the University of Windsor.

(1) Murray, S. G.; Hartley, F. R. *Chem. Rev.* **1981**, *81*, 365-414 and references cited therein.
(2) Cooper, S. R. *Acc. Chem. Res.* **1988**, *21*, 141-146 and references cited therein.
(3) Loeb, S. J.; de Groot, B. *Inorg. Chem.* **1989**, *28*, 3573-3578.
(4) Wolf, R. E.; Hartman, J. R.; Storey, J. M. E.; Foxman, B. M.; Cooper, S. R. *J. Am. Chem. Soc.* **1987**, *109*, 4328-4335.
(5) Yoshida, T.; Adachi, T.; Ueda, T.; Watanabe, M.; Kaminaka, M.; Higuchi, T. *Angew. Chem., Int. Ed. Engl.* **1987**, *26*, 1171-1172.
(6) Schröder, M. *Pure Appl. Chem.* **1988**, *60*, 517-524 and references cited therein.
(7) Blake, A. J.; Gould, R. O.; Reid, G.; Schröder, M. *J. Organomet. Chem.* **1988**, *356*, 389-396.

0020-1669/90/1329-4084$02.50/0